

THE EFFECT OF POLYETHYLENE GLYCOL (PEG) COATING ON THE MAGNETO-STRUCTURAL PROPERTIES AND COLLOIDAL STABILITY OF $\text{Co}_{0.8}\text{Mg}_{0.2}\text{Fe}_2\text{O}_4$ NANOPARTICLES FOR POTENTIAL BIOMEDICAL APPLICATIONS

C. O. EHI-EROMOSELE^{a*}, B. I. ITA^{a,b}, E. E. J. IWEALA^c

^a*Department of Chemistry, Covenant University, PMB 1023, Ota, Nigeria.*

^b*Department of Pure and Applied Chemistry, University of Calabar, Calabar, Nigeria*

^c*Department of Biological Sciences, Covenant University, PMB 1023, Ota, Nigeria*

The effect of polyethylene glycol (PEG) coating on the magneto-structural properties and colloidal stability of $\text{Co}_{0.8}\text{Mg}_{0.2}\text{Fe}_2\text{O}_4$ magnetic nanoparticles (MNPs) was studied with their potential biomedical applications in mind using powder X-ray diffraction (XRD), Field Emission Scanning Electron Microscope (FESEM), vibrating sample magnetometer (VSM) and zeta potential measurements. $\text{Co}_{0.8}\text{Mg}_{0.2}\text{Fe}_2\text{O}_4$ MNPs were synthesized by a two-step chemical method including solution combustion synthesis followed by functionalisation with PEG. The XRD patterns indicate that the crystalline single phase cubic spinel structure was retained after PEG coating. Also, after PEG coating, the crystallite size (from Scherrer formula) increases from 50 to 56 nm. Magnetic measurements of both coated and uncoated particles reveal the ferrimagnetic nature at room temperature with the PEG coated sample recording a higher magnetic moment. The resulting PEG coated particles form a more stable suspension in aqueous environment and also an appreciable stability in phosphate buffer solution (PBS) at physiological pH. The higher magnetization and colloidal stability recorded with PEG coatings is an important parameter in biomedical applications.

(Received November 2, 2015; Accepted January 4, 2016)

Keywords: Magnetic nanoparticles; Combustion synthesis; Magnetic hyperthermia; Colloidal stability; PEG

1. Introduction

Nanotechnology is a frontier in science, engineering and manufacturing which has introduced new opportunities for the improvement of medical treatment. The application of nanotechnology to medicine, known as nanomedicine, concerns the use of precisely engineered materials at the molecular scale to develop novel therapeutic and diagnostic devices generally encompassing 1–500 nm [1-3]. Magnetic nanoparticles (MNPs) are one of the important sub-classes of nanomaterials applied in cancer diagnosis and therapy [4]. In the past few years, MNPs have been mainly used as heat sources in the treatment of tumors by hyperthermia and as nanovectors for controlled drug delivery [5,6].

Ferrite nanoparticles are well suited for biomedical applications because their sizes can be manipulated and also their surface can be functionalised with appropriate molecules to make them highly selective towards their targets [7,8]. The use of iron oxide (magnetite) nanoparticles such as Fe_3O_4 and substituted iron oxides (MFe_2O_4 where M = Co, Mn, Zn, Mg etc.) for biomedical applications has been studied extensively [9]. Superparamagnetic iron oxide nanoparticles have

*Corresponding author: cyril.ehi-eromosele@covenantuniversity.edu.ng

been the most appealing because of their biocompatibility, enhanced specific loss power and easy functionalisation. However, it has been found that in most recent clinical trials of local hyperthermia, for example, a large dose (milligram-level) of these nanoparticles are required to be injected into the tumour due to the low energy conversion efficiency of such ultra-small MNPs [10]. Hence, the selection of the most advantageous materials for clinical hyperthermia treatment, as well as other biomedical applications, is still a matter of debate [11]. One strategy used in the design of magnetic core for biomedical applications is the synthesis of mixed ferrites, where simple ferrites with one type of magnetic ion (excluding iron) are doped with other kinds of ion. This is done to utilise the different outstanding features of different ions [12]. Here, 20% of magnesium ions were used to dope cobalt ferrite for the exploitation of its potentials in magnetic hyperthermia. Cobalt ferrite (CoFe_2O_4) nanoparticles have a high saturation magnetization and magnetic anisotropy which improves the heat transfer rate. In biomedical applications, these are the properties desired when MNPs are to be used as heating mediators in hyperthermia treatments and as drug carriers since they can be easily manipulated by an applied magnetic field. And MgFe_2O_4 nanoparticles have been shown to be toxic towards cancer cells [13].

Nanoparticles have hydrophobic surfaces with large surface to volume ratio hence the particles get agglomerated and form clusters that can easily adsorb plasma proteins. So, to prevent opsonisation and avoid macrophage recognition leading to the clearance of the MNPs, surface coating of the MNPs is required. The coating can consist of long-chain organic ligands or inorganic/organic polymers, where these ligands or polymers can be introduced during (in-situ coating) or after (post-synthetic coating) synthesis. PEG coated MNPs reveal excellent stability and solubility in aqueous dispersions and in physiological media [14]. PEG coatings have been used to reduce phagocytic capture of nanoparticles by the immune system, which can extend nanoparticle circulation time and subsequent accumulation in targeted tissue [15]. PEG shell does not seem to affect the thermal characteristics and might make the magnetic fluid useful for hyperthermia treatment [16].

All biomedical applications of MNPs require that the nanoparticles have high magnetization values, with sizes smaller than 100 nm, and a narrow particle size distribution [17] which are all highly sensitive to synthesis methods. There are different methods of synthesis of ferrites which includes chemical co-precipitation and combustion methods. Although, chemical co-precipitation method is suitable for mass production of MNPs, it does require careful adjustment of pH. Combustion method is known for its cost effectiveness, low reaction time, large mass production and homogeneity among the products [18]. Also, no further thermal treatment is required for samples prepared by combustion method [19]. Therefore, the current study is about the solution combustion synthesis of nanocrystalline $\text{Co}_{0.8}\text{Mg}_{0.2}\text{Fe}_2\text{O}_4$ using glycine-nitrate mixture precursors which was subsequently stabilized with PEG. Since the coating of polymers on the surface of MNPs can alter some important properties of the particles, the effect of PEG coatings on the structural, morphological and magnetic properties are discussed in detail. The colloidal stability of bare and PEG coated $\text{Co}_{0.8}\text{Mg}_{0.2}\text{Fe}_2\text{O}_4$ MNPs in water was examined. The colloidal stability of PEG coated $\text{Co}_{0.8}\text{Mg}_{0.2}\text{Fe}_2\text{O}_4$ MNPs in phosphate buffer solution (PBS) at pH 7.4 (physiological pH) and pH 5.0 (cancer cell endosomal pH) was also studied to highlight its stability in different physiological media.

2. Experimental

2.1 Materials

Analytical grade $\text{Co}(\text{NO}_3)_2 \cdot 6\text{H}_2\text{O}$ (99 % purity of Sigma-Aldrich), $\text{Mg}(\text{NO}_3)_2 \cdot 6\text{H}_2\text{O}$ (99% purity of Alfar Aesar), $\text{Fe}(\text{NO}_3)_3 \cdot 9\text{H}_2\text{O}$ (99% purity of Sigma Aldrich) were taken as oxidants, while glycine (G, $\text{C}_2\text{H}_5\text{NO}_2$) obtained from SD Fine Chem. Ltd., Mumbai, was employed as fuel to drive the combustion process. Polyethylene glycol (PEG-6000, MW: 5000-7000) obtained from Spectrochem, India was used for the surface coating of nanoparticles. Double distilled water was used throughout the experiments. All reagents were used without further purification.

2.2 Synthesis of $\text{Co}_{0.8}\text{Mg}_{0.2}\text{Fe}_2\text{O}_4$ MNPs

$\text{Co}_{0.8}\text{Mg}_{0.2}\text{Fe}_2\text{O}_4$ MNPs were prepared by the solution combustion method using fuel rich glycine-nitrate (G/N = 2.22) composition. The optimization of the crystallinity and particle size of $\text{Co}_{0.8}\text{Mg}_{0.2}\text{Fe}_2\text{O}_4$ MNPs using fuel to oxidizer ratio and sintering temperature has been studied in detail in our recent publication [20]. Appropriate amounts of $\text{Co}(\text{NO}_3)_2 \cdot 6\text{H}_2\text{O}$, $\text{Mg}(\text{NO}_3)_2 \cdot 6\text{H}_2\text{O}$, $\text{Fe}(\text{NO}_3)_3 \cdot 9\text{H}_2\text{O}$, and $\text{C}_2\text{H}_5\text{NO}_2$ were dissolved in 20 ml of de-ionised water. Then the solutions were heated to 80°C to form a viscous gel of precursors under magnetic stirring. Secondly, the gel was transferred to a pre-heated coil (300°C). Finally, after a short moment, the solution precursors boiled, swelled, evolved a large amount of gases and ignited, followed by the yielding of puffy black products. The auto-combusted powder was used further for PEG coating without any subsequent annealing process.

2.3 Synthesis of PEG Coated $\text{Co}_{0.8}\text{Mg}_{0.2}\text{Fe}_2\text{O}_4$ MNPs

The MNPs were coated with PEG following the method [21] but with some modifications. Aqueous PEG solution (2% w/v) was prepared. The mixture of 100 mg $\text{Co}_{0.8}\text{Mg}_{0.2}\text{Fe}_2\text{O}_4$ MNPs and distilled water (100 mL) were homogenized by ultrasonication for 30 min. Then the aqueous solution of PEG was added to the suspension of $\text{Co}_{0.8}\text{Mg}_{0.2}\text{Fe}_2\text{O}_4$ in water with slow agitation. After stirring for 24 hrs, the mixture of MNPs and PEG was washed three times with distilled water to remove excess PEG and then dried at 60°C for 1 hr.

2.4 Characterization

The X-ray diffractograms of the uncoated and PEG coated MNPs were recorded using an X-ray diffractometer (D8 Advance, Bruker, Germany), equipped with a $\text{Cu K}\alpha$ radiation source ($\lambda = 1.5406 \text{ \AA}$) and the crystallite size was calculated by the well-known Debye-Scherrer relation.

$$D = \frac{0.9\lambda}{\beta \cos\theta} \quad (1)$$

where β is the full-width at half maxima (in radians) of the strongest intensity diffraction peak (311), λ is the wavelength of the radiation and θ is the angle of the strongest characteristic peak. Eq. 2. was employed to calculate the lattice parameter (a) using the value of d-spacing of the strongest intensity diffraction peak.

$$a = d_{hkl} \sqrt{h^2 + k^2 + l^2} \quad (2)$$

where, h, k, l are the Miller indices of the crystal planes and d_{hkl} is the separation of lattice planes X-ray density (D_x) was calculated using equation 3.

$$D_x = \frac{8M}{Na^3} \quad (3)$$

Where, M is the molecular weight, N is the Avogadro's number, and a, is the lattice constant. The surface morphology of the uncoated and PEG coated MNPs was examined with a Field Emission-Scanning Electron Microscopes, Nova Nano SEM 600 (FEI Co., Netherlands). The magnetic characterizations were carried out with a Vibrating Scanning Magnetometer (Lake Shore cryotronics-7400 series) under the applied field of $\pm 20,000 \text{ G}$ at room temperature. Zeta potential measurements were performed using a zeta sizer (Nano Zs, Nano series Malvern instruments). Measurements were taken in water and in PBS. Zeta potential measurements were done thrice for each sample at 30 electrode cycles.

3. Results and Discussion

3.1 Coating of $\text{Co}_{0.8}\text{Mg}_{0.2}\text{Fe}_2\text{O}_4$ sample with PEG

PEG was employed to coat the $\text{Co}_{0.8}\text{Mg}_{0.2}\text{Fe}_2\text{O}_4$ MNPs to improve its biocompatibility and colloidal stability for biological applications. PEG is a neutral, hydrophilic, linear synthetic polymer that shows excellent stability and solubility in aqueous dispersions and in physiological media. Fig. 1 shows a schematic representation of the coating of $\text{Co}_{0.8}\text{Mg}_{0.2}\text{Fe}_2\text{O}_4$ MNPs with PEG.

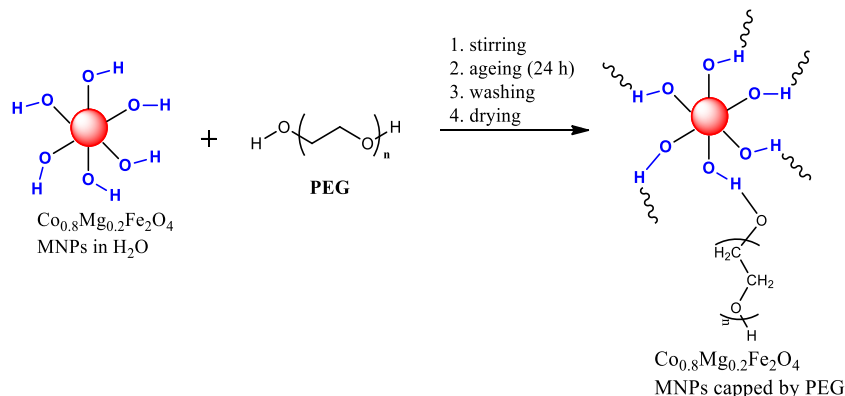


Fig. 1: Schematic representation of the coating of $\text{Co}_{0.8}\text{Mg}_{0.2}\text{Fe}_2\text{O}_4$ MNPs with PEG

3.2 Structural and Phase Analysis of PEG Coated $\text{Co}_{0.8}\text{Mg}_{0.2}\text{Fe}_2\text{O}_4$ MNPs

The XRD patterns of PEG coated nanocrystalline $\text{Co}_{0.8}\text{Mg}_{0.2}\text{Fe}_2\text{O}_4$ sample is shown in Fig. 2. The effects of PEG coating on the structural properties of $\text{Co}_{0.8}\text{Mg}_{0.2}\text{Fe}_2\text{O}_4$ MNPs are presented in Table 1. Like the XRD of the uncoated sample, the diffraction peaks has the characteristic peaks of a single phase spinel cubic structure (JCPDS card no.22-1086). This clearly showed that the sample retained the spinel structure even after coating with PEG but with a suppression of diffraction peaks apparently due to the presence of PEG coatings. PEG can induce internal strain due to lattice mismatch i.e. lattice strain between polymer and MNPs at the interface which results readily in the decrease of the intensity of peaks [22]. There is a pronounced change in the calculated structural properties of coated sample compared to the uncoated sample with the coated sample recording higher values of all calculated structural properties than the uncoated sample. The calculated crystallite sizes (D) for uncoated and coated MNPs are 50 nm and 56 nm, respectively (Table 1). The increase in the calculated crystallite size which had also caused the increase in other structural properties might be due to the presence of PEG coating. It is likely that in the presence of PEG, small particles have tendency to join together and constitute large particles. The increase in crystallite size with polymer coating (PVA) has been reported for $\text{Ni}_{0.3}\text{Zn}_{0.7}\text{Fe}_2\text{O}_4$ MNPs [23].

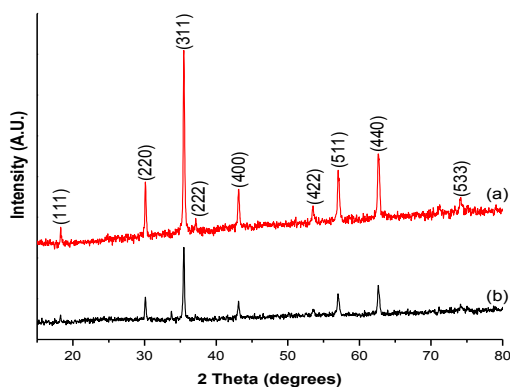


Fig. 2: X-ray diffraction patterns of (a) uncoated and (b) PEG coated $\text{Co}_{0.8}\text{Mg}_{0.2}\text{Fe}_2\text{O}_4$ MNPs

Table 1: Effects of PEG Coating on the Structural Properties of $\text{Co}_{0.8}\text{Mg}_{0.2}\text{Fe}_2\text{O}_4$ MNPs

$\text{Co}_{0.8}\text{Mg}_{0.2}\text{Fe}_2\text{O}_4$ MNPs	Crystallite size, D, (nm)	Lattice constant, a, (nm)	Unit cell volume, V, nm^3	X-ray density, D_x , g/cm^3
Uncoated	50	0.838	0.589	5.140
PEG coated	56	0.840	0.593	6.090

3.3 Morphological Analysis of PEG Coated $\text{Co}_{0.8}\text{Mg}_{0.2}\text{Fe}_2\text{O}_4$ MNPs

Fig. 3 shows typical FE-SEM images of uncoated and PEG coated $\text{Co}_{0.8}\text{Mg}_{0.2}\text{Fe}_2\text{O}_4$ MNPs. It can be seen from Fig. 3 that there is an enlargement of $\text{Co}_{0.8}\text{Mg}_{0.2}\text{Fe}_2\text{O}_4$ particles after PEG coating. Therefore, FE-SEM images confirm the XRD data regarding enlarging particles by PEG coating. As stated earlier, in the presence of PEG, small particles have tendency to join together and constitute large particles. Also, it can be observed from the FE-SEM images that the uncoated samples are in highly agglomerated form while the PEG coated sample displays much better dispersion. Enhancement in dispersibility after coating may be attributed to the presence of the non-magnetic surface layer of PEG which readily decreases the interparticle interaction.

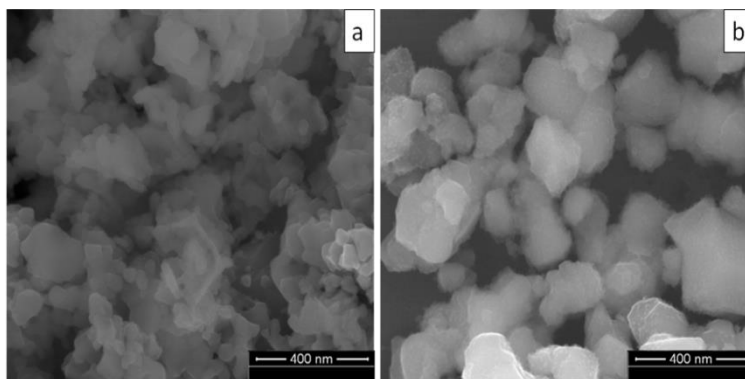


Fig. 3: FESEM images of $\text{Co}_{0.8}\text{Mg}_{0.2}\text{Fe}_2\text{O}_4$ samples (a) uncoated (b) PEG coated

3.4 Magnetic Properties of PEG Coated $\text{Co}_{0.8}\text{Mg}_{0.2}\text{Fe}_2\text{O}_4$ MNPs

The hysteresis loops measured at room temperature for the uncoated and PEG coated $\text{Co}_{0.8}\text{Mg}_{0.2}\text{Fe}_2\text{O}_4$ MNPs are shown in Fig. 4. The magnetic results show that $\text{Co}_{0.8}\text{Mg}_{0.2}\text{Fe}_2\text{O}_4$ MNPs (uncoated and PEG coated) is ferrimagnetic at room temperature. The saturation magnetization (M_s), remanence (M_r), coercivity (H_c) and loop squareness ratio (M_r/M_s) of the uncoated and coated sample are summarized in Table 2. The coated sample had a higher M_s , M_r and H_c but a lower M_r/M_s values than the uncoated sample. It can be seen that the M_s of the coated sample (61 emu/g) is higher than the uncoated sample (55 emu/g) at an applied field of $\pm 20,000$ G at 300 K. The increase in magnetization of the coated sample is probably due to the nanoparticles' crystal growth (which is evident from the XRD result) after polymer coating. So the values of M_s are in accordance with the amount of magnetic substance in each material per gram. The increase in magnetization might be also due to spin injection or anti-spin canting being transpired at the surfaces of the MNPs due to the interaction with polymer chain [24]. Depending on the applications, certain properties of MNP are desired. In most biomedical applications, nanoparticles with higher saturation magnetization are preferred because they provide higher sensitivity and efficiency [25]. It can be seen that the PEG coatings conferred higher magnetization on the MNPs thereby enhancing their applications as heating foci in hyperthermia applications. The heating efficiency of hyperthermia nanomaterials obtained by measuring the specific loss power (SLP) is usually proportional to the M_s and H_c of the nanoparticles [26]. However, it is important to note that the heating efficiency of MNPs depends on many other factors such as particle size, shape, morphology as well as on extrinsic parameters like the applied AC magnetic field [27].

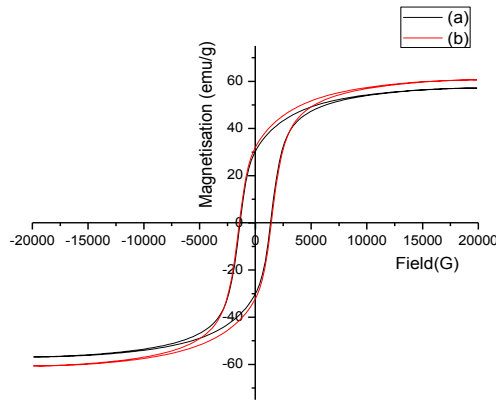


Fig. 4: Magnetic hysteresis curves of $Co_{0.8}Mg_{0.2}Fe_2O_4$ (auto-combusted) measured at room temperature for (a) the uncoated sample (b) the PEG coated sample

Table 2: Magnetic Properties of the Uncoated and the PEG Coated $Co_{0.8}Mg_{0.2}Fe_2O_4$ MNPs

Sample	Saturation Magnetisation, M_s (emu/g)	Remanence Magnetisation, M_r (emu/g)	Coercivity (Gauss)	M_r/M_s
Uncoated sample	55	30	1200	0.55
PEG coated sample	61	33	1489	0.54

3.5 Colloidal Stability of PEG Coated $Co_{0.8}Mg_{0.2}Fe_2O_4$ MNPs

The colloidal stability of the uncoated and PEG coated sample was evaluated by zeta potential measurements. The zeta potential distribution of uncoated and coated sample using distilled water as a dispersant is shown in Fig. 5. The zeta potential value in distilled water observed for the coated sample (-11.55 mV) is higher than the uncoated sample (-8.26 mV). This result shows that there is lesser aggregation of the coated sample in water compared to the uncoated sample. High charge differences ($> \pm 10$ mV) lead to greater interparticle repulsion [28] hence, there is enhancement of colloidal stability with increasing zeta potential values. Solubility in aqueous medium like water increases due to the hydrophilic ethylene glycol repeats in the PEG coating. Colloidal stability in aqueous as well as in physiological media like PBS is required for MNPs to be successfully applied in biomedical applications like magnetic fluid hyperthermia. The zeta potentials of the PEG coated sample is -14.00 mV at pH 7.4 (physiological pH) and -8.45 mV at pH 5.0 (cancer cell endosomal pH). At pH 7.4, more of the hydroxyl end groups will be ionized making it more negatively charged. At pH 5, the hydroxyl end group ionization is lesser thus lowering the net negative charge. The results show that the PEG coated $Co_{0.8}Mg_{0.2}Fe_2O_4$ MNPs are relatively colloidally stable both in aqueous and physiological environments. These results imply that the PEG coated $Co_{0.8}Mg_{0.2}Fe_2O_4$ NPs could maintain their dispersion stability and heating capacity in various physiological environments and thus have great potentials to be used in biomedical applications.

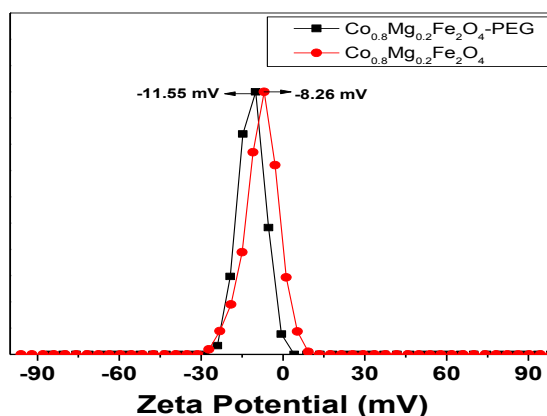


Fig. 5: Zeta potential distribution of bare and PEG coated $\text{Co}_{0.8}\text{Mg}_{0.2}\text{Fe}_2\text{O}_4$ nanoparticles using distilled water as dispersant

4. Conclusion

The single cubic spinel phase of nanocrystalline $\text{Co}_{0.8}\text{Mg}_{0.2}\text{Fe}_2\text{O}_4$ MNPs was obtained by the glycine mediated combustion synthesis with no further heat treatment. The surfaces of the synthesized MNPs were functionalized with PEG thereby conferring suitable chemical, physical and physiological properties for magnetic hyperthermia applications. From XRD, PEG coated sample retained their crystalline structure but with a slight suppression of peaks and crystallite size increased after coating. PEG coated $\text{Co}_{0.8}\text{Mg}_{0.2}\text{Fe}_2\text{O}_4$ MNPs recorded an increase in the structural and magnetic properties compared with the uncoated sample. The increase in structural properties was attributed to the tendency of small particles to join together and constitute large particles in the presence of PEG which also might have accounted for the increase in magnetic properties. There was improved colloidal stability with PEG coating in aqueous medium and also an appreciable stability in PBS at physiological pH highlighting the favourable potential biomedical applications of PEG coated $\text{Co}_{0.8}\text{Mg}_{0.2}\text{Fe}_2\text{O}_4$ MNPs.

Acknowledgements

This work would not have been possible without the visiting research grant given to Dr. Ehi-Eromosele C.O. by the International Centre for Materials Science, Jawaharlal Nehru Centre for Advanced Scientific Research, Bangalore, India.

References

- [1] O.C. Farokhzad, R. Langer, *Advanced Drug Delivery Reviews* **58**, 1456 (2006).
- [2] Y. Liu, H. Miyoshi, M. Nakamura, *International Journal of Cancer* **120**, 2527 (2007).
- [3] L. Zhang, F.X. Gu, J.M. Chan, A.Z. Wang, R.S. Langer, O.C. Farokhzad, *Clinical Pharmacology and Therapeutics* **83**(5),761 (2008).
- [4] A.B. Salunkhe, V.M. Khot, S.H. Pawar, *Current Topics in Medicinal Chemistry* **14**(5), 572 (2014).
- [5] M. Kallumadil, M. Tada, T. Nakagawa, M. Abe, P. Southern, Q. A. Pankhurst, J. Magn. Mater.**321**, 1509 (2009).
- [6] S. S. Banerjee, D. H. Chen, *Chem. Mater.***19**, 6345 (2007)
- [7] D.L. Leslie-Pelecky, R.D. Rieke, *Chem. Mater.* **8**, 1770 (1996).
- [8] T. Suzuki, M. Shinkai, M. Kamihira, M. Kobayashi, *Biotechnol. Appl. Biochem.* **21**, 335 (1995).

- [9] S. Laurent, D. Forge, M. Port, A. Roch, C. Robic, L. Vander Elst, R.N. Muller, *Chem. Rev.* **108**, 2064 (2008).
- [10] K. Maier-Hauff, F. Uldrich, D. Nestler, H. Niehoff, P. Wust, B. Thiesen, H. Orawa, V. Budach, A. Jordan, *J. Neuro-Oncol.* **103**, 317 (2011).
- [11] C.S.S.R. Kumar, F. Mohammad, *Adv. Drug Deliver. Rev.* **63**, 789 (2011).
- [12] R. Arulmurugan, B. Jeyadevan, G. Vaidyanathan, S. Sendhilnathan, *J. Magn. Magn. Mater.* **288**, 470 (2005).
- [13] S. Kanagesan, M. Hashim, S. Tamilselvan, N.B. Alitheen, I. Ismail, G. Bahmanrokh, *Journal of Nanomaterials*, 1(2013).
- [14] E. Umut, *Surface Modification of Nanoparticles used in Biomedical Applications In: Modern Surface Engineering Treatments*, Ed. by Mahmood Aliofkhaezrai. InTech 185-208 (2013).
- [15] E.K.U. Larsen, T. Nielsen, T. Wittenborn, H. Birkedal, T. Vorup-Jensen, M.H. Jakobsen, L. Østergaard, M.R. Horsman, F. Besenbacher, K.A. Howard, J. Kjems, *ACS Nano* **3**, 1947 (2009).
- [16] V.M. Khot, A.B. Salunkhe, J.M. Ruso, S.H. Pawar, *J. Magn. Magn. Mater.* **384**, 335 (2015).
- [17] A.S. Teja, P.Y. Koh, *Prog. Cryst. Growth. Character.* **55**, 22(2009).
- [18] V.M. Khot, A.B. Salunkhe, N.D. Thorat, M.R. Phadatore, S.H. Pawar, *J. Magn. Magn. Mater.* **332**, 48 (2013).
- [19] M. Syue, F. Wei, C. Chou, C. Fu, *Journal of Applied Physics* **109**, 07A324 (2011).
<http://dx.doi.org/10.1063/1.3560880>.
- [20] C.O. Ehi-Eromosele, B.I. Ita, E.E.J. Iweala, *Journal of Sol-Gel Science and Technology* **76**(2), 298 (2015).
- [21] M.R. Phadatore, V.M. Khot, A.B. Salunkhe, N.D. Thorat, S.H. Pawar, *J. Magn. Magn. Mater.* **324**, 770 (2012).
- [22] S.V. Jadhav, D.S. Nikam, V.M. Khot, S.S. Mali, C.K. Hong, S.H. Pawar, *Materials Characterization* **102**, 209 (2015).
- [23] M. Rahimi, P. Kameli, M. Ranjbar, H. Salamati, *J. Magn. Magn. Mater.* **347**, 139(2013).
- [24] A.S. Prasad, S.N. Dolia, *J. Magn. Magn. Mater.* **324**, 869 (2012).
- [25] M. Colombo, S. Carregal-Romero, M.F. Casula, L. Gutierrez, M.P. Morales, I.B. Bohm,
- [26] J.T. Heverhagen, D. Prospero, W.J. Parak, *Chem. Soc. Rev.* **41**, 4306(2012).
- [27] D. Sakellari, K. Brintakis, A. Kostopoulou, E. Myrovali, K. Simeonidis, A. Lappas, M. Angelakeris, *Materials Science and Engineering C* **58**, 187 (2016).
- [28] G. Salas, S. Veintemillas-Verdaguer, M.P. Morales, *Int. J. Hyperth.* **29**, 768 (2013).
- [29] J.V. Jokerst, T. Lobovkina, R.N. Zare, S.S. Gambhir, *Nanomedicine* **6**(4), 715 (2011).